Synthesis, Characterization and Catalysis of Ce-MCM-41

Shu-Hua Chien[a,b]* (簡淑華), Ming-Chih Kuo[a] (郭明智) and Chun-Long Chen[a,b] (陳春龍)
[a]*Institute of Chemistry, Academia Sinica, Taipei 11529, Taiwan, R.O.C.*
[b]*Department of Chemistry, National Taiwan University, Taipei 10674, Taiwan, R.O.C.*

The cerium-containing MCM-41 (Ce-MCM-41) has been synthesized by direct hydrothermal method. The low-angle XRD patterns revealed the typical five major peaks of MCM-41 type hexagonal structures. The interplanar spacing d_{100} = 38.4 Å was obtained that can be indexed on a hexagonal unit cell parameter with a_o = 44.3 Å which was larger than that of pure siliceous MCM-41 (Si-MCM-41). Transmission electron micrograph shows the regular hexagonal array of uniform channel characteristics of MCM-41. The BET surface area of Ce-MCM-41 was 840 m^2/g, which is much reduced as compared to that of Si-MCM-41, with the pore size of 26.9 Å and mesopore volume of 0.78 cm^3/g were measured by nitrogen adsorption-desorption isotherm at 77 K. Along with the results, the synthesized Ce-MCM-41 exhibited a well-ordered MCM-41-type mesoporous structure with the incorporation of cerium. Using Ce-MCM-41 as a support, the Rh (0.5 wt%) catalyst exhibited very high activity for the NO/CO reactions.

Keywords: Cerium-containing MCM-41; Rh catalyst; In-situ FT-IR; NO/CO reactions.

INTRODUCTION

Zeolites and related molecular sieves have been extensively investigated for various catalytic applications due to their unique structural and textural properties.[1-3] Since M41S mesoporous molecular sieves were first reported by the Mobil group in 1992,[4,5] the synthesis, characterization and potential applications for adsorption, separation and catalysis of mesoporous materials have been widely investigated.[3] MCM-41 exhibits a highly ordered hexagonal array of one-dimensional mesopores, whose diameters can be varied from 15 to 100 Å with a narrow pore-size distribution through the adequate surfactant as the template and synthetic condition.[3-10] The modification of MCM-41 through incorporating the divalent, trivalent, tetravalent transition and nontransition metal ions as well as the lanthanide metals in the silica network of MCM-41 materials has been reported.[1,11-19] Lanthanide-incorporated mesoporous silicates showed an improvement in their thermal stability and structural properties such as the pore volume and surface area in comparison to pure MCM-41.

Cerium oxide is well-known in automotive three-way catalytic converters as an oxygen storage medium and thermal stabilizer.[20-24] In the present study, Ce-containing MCM-41 with thermal stability, high surface area and mesoporous structure was synthesized by direct hydrothermal method. The structural characterization of the resulting molecular sieves was well investigated by various physicochemical and spectroscopic methods. It is also evident that with Ce-MCM-41, the impregnated Rh catalyst exhibits high activity in NO/CO reactions.

EXPERIMENTAL

Synthesis of cerium-containing and pure Si (siliceous) MCM-41

The Ce-containing MCM-41 (Ce-MCM-41) was synthesized by direct hydrothermal method modifying the methods reported by Beck et al.[4,5] and Lin et al.[7-10] Briefly, an aqueous solution of cerium nitrate was added to an aqueous solution of CTABr ($C_{16}H_{33}N(CH_3)_3Br$), and then sodium silicate was added. The pH value of the mixture was adjusted to 10 by adding 1 M H_2SO_4 in a dropwise manner. The gel was transferred to a Teflon-lined stainless steel autoclave and placed in an oven at 100 °C for 6 days under static hydrothermal conditions. After quick cooling the autoclave, the solid sample was centrifuged, washed and dried; then it was calcined at 540 °C in N_2 for 1 hour and subsequently in air for 6

Dedicated to Professor Ching-Erh Lin on the Occasion of his 66th Birthday and his Retirement from National Taiwan University

* Corresponding author. Tel: +886-2-2789-8528; Fax: +886-2-2783-1237; E-mail: chiensh@gate.sinica.edu.tw

hours. For comparison, pure Si or the siliceous-MCM-41 (Si-MCM-41) was synthesized in the same manner except no cerium nitrate was added.

Characterization of the synthesized Ce-MCM-41

Thermal analysis of the as-synthesized MCM-41 was carried out in nitrogen with a flow rate of 25 cm^3/min and taken with a Du Pont TGA 951 Thermogravimetric Analyzer. The inductively coupled plasma-mass spectrometry (ICP-Mass) analysis of the calcined MCM-41 was performed on a Sciex Elan 5000 spectrometer (Perkin Elmer). The surface area of the prepared molecular sieves was determined by the Brunauer-Emmett-Teller (BET) method and the pore size distribution by the Barrett-Joyner-Halenda (BJH) method applied to the adsorption curve using a Micromeritics ASAP 2010 surface area analyzer. The powder X-ray diffraction (XRD) measurements were performed on a Siemens D5000 diffractometer with nickel-filtered Cu Kα radiation. Transmission and scanning electron microscope (TEM and SEM) were carried out on Hitachi H-7000 TEM and S-800 SEM systems, respectively. Diffuse reflectance UV-visible (UV-vis) spectra were taken on a Hitachi U-3410 spectrometer with a 60Φ integrating sphere accessory. Infrared spectra were obtained with a Bomem DA-8 FT-IR spectrometer. The acidity of the prepared samples was investigated by in-situ FT-IR spectroscopic studies of pyridine adsorption. The IR-cell used in the present study is the same as described previously.[25] The solid-state ^{29}Si MAS-NMR spectra were acquired on Bruker MSL-200 and MSL-500 spectrometers with commercial magic angle spinning (MAS) probes.

Measurements of catalytic activity for NO/CO reactions

The measurements of the activities and selectivities for the NO/CO reactions were carried out in a flow-mode microreactor system operating at atmospheric pressure with a flow-rate ratio of NO/CO = 1. Both gases are 4% content in He and the flow rates were maintained at 10 cm^3/min. The exit gases were analyzed by an on-line Varian 3700 gas chromatograph with two columns connected in series: a 12 ft Porapak Q and a 30 ft GasChrom MP-1 (both in 1/8" stainless steel tubings). The columns were heated at 40 °C for 10 min and then heated to 150 °C at a rate of 10 °C/min. A TCD detector and a quadrupole mass spectrometer were simultaneously used to measure the reaction products. The TCD peak area was determined by a Perkin Elmer Nelson 1022 integrator and calibrated with known gaseous molecules.

In-situ FT-IR spectroscopy

Adsorption and interaction of CO and NO were investigated by in-situ FT-IR spectroscopy on thin self-supporting catalyst wafers (20-30 mg/cm^2) in a quartz high-vacuum IR cell under 1-3 torr of adsorbate gases. In-situ infrared spectra were taken on a Bomem DA-8 FT-IR spectrometer.

RESULTS AND DISCUSSION

The cerium-containing MCM-41 molecular sieve (Ce-MCM-41) was synthesized by direct hydrothermal method. Thermogravimetric analysis (TGA) and the corresponding first derivative curves (DTG) of as-synthesized Ce-MCM-41 and Si-MCM-41 were carried out to understand the weight change of samples as a function of temperature. Both TGA curves could mainly be divided into 3 weight loss steps which agreed with the results in the literature.[12,14,16,24] The step below 150 °C is ascribed to the desorption of physically adsorbed water. The step between 150-310 °C with a DTG peak at around 265 °C and a shoulder at around 173 °C is due to the desorption and/or decomposition of the template.[15,18,26] The relative small weight loss step appearing above 310 °C is ascribed to the condensation of silanol groups for forming water. For Ce-MCM-41, the weight loss caused by the condensation of silanols is greater than that of Si-MCM-41 and the corresponding DTG peak shifts to the high temperature side. It has been reported that the as-synthesized Ce-MCM-41 sample containing hydrated cerium species could decompose during calcination:[15,18] Ce^{4+}-(H_2O) → Ce^{3+}-OH + H^+. The Ce^{3+}-OH species possibly acts as the Lewis acid sites on the surface of catalyst. The results indicated that the stronger Lewis acidity was formed on Ce-MCM-41 in this temperature region. Accordingly, the calcination of the as-synthesized template-containing MCM-41 was performed at 540 °C in nitrogen for 1 hour and in air for 6 hours in either case, which led to the removal of adsorbed water and template, as well as the condensation of silanols.

Fig. 1 shows the powder X-ray diffraction (XRD) patterns of synthesized Ce-MCM-41 and Si-MCM-41 before and after calcination. The XRD patterns show significant shifts on peak position after calcination due to the cell contraction in comparison with that of the as-synthesized samples. The XRD pattern of Ce-MCM-41 indeed reveals a well-defined MCM-41 crystalline structure with five peaks appearing in the low-angle pattern. An interplanar spacing

Table 1. Nitrogen adsorption parameters of Ce-MCM-41 and Si-MCM-41

Molecular sieve	surface area (m^2/g)	pore volume (cm^3/g)	pore size (Å)	wall thickness (Å)
Ce-MCM-41	840	0.78	26.9	17.4
Si-MCM-41	1267	1.11	25.0	16.5

d_{100} = 40.58 Å was obtained for Ce-MCM-41 and d_{100} = 38.55 Å for Si-MCM-41 before calcinations; they can be indexed on a hexagonal unit cell with $a_o = (2d_{100}/\sqrt{3})$ = 46.86 Å and 44.51 Å, respectively. Apparently, a_o value of Ce-MCM-41 is larger than the pure siliceous counterparts (Si-MCM-41). After calcination, a cell contraction of 2.6 Å was obtained for Ce-MCM-41 and 3.1 Å for Si-MCM-41. The results indicated that the incorporation of Ce led to a larger hexagonal unit cell parameter and a milder cell contraction during calcination.

N_2 adsorption-desorption isotherm at 77 K and the corresponding pore size distribution curve (inset) of Ce-MCM-41 and Si-MCM-41 are shown in Fig. 2. Ce-MCM-41 presents a similar isotherm with Si-MCM-41. In the relative pressure range between 0.3 and 0.4 for Ce-MCM-41, the step is not as sharp as that for Si-MCM-41. N_2 adsorption-desorption isotherms indicated surface areas of 840 m^2/g and 1267 m^2/g and pore sizes 26.9 Å and 25.0 Å for Ce-MCM-41 and Si-MCM-41, respectively. The wall thicknesses of 17.4 Å and 16.5 Å were calculated by (a_o - pore size) for Ce-MCM-41 and Si-MCM-41, respectively, as listed in Table 1. The results indicated that the incorporation of Ce in MCM-41 not only led to the increase in unit cell parameter, but also enlarged the pore diameter. The effect of Ce incorporation on the MCM-41 structure is opposite to that of Al species,[9] which could be attributed to the atomic size of Ce being greater than that of Si.

From ICP-Mass results, the calcined sample contains 3.3 wt% Ce with an atomic ratio of Ce/Si = 1/67.6. It was noticed that about 88.8% of Ce in gel (Ce/Si = 1/60) was well incorporated into the synthesized sample by the present hydrothermal synthesis method.

Fig. 3(a) shows the TEM morphology of Ce-MCM-41;

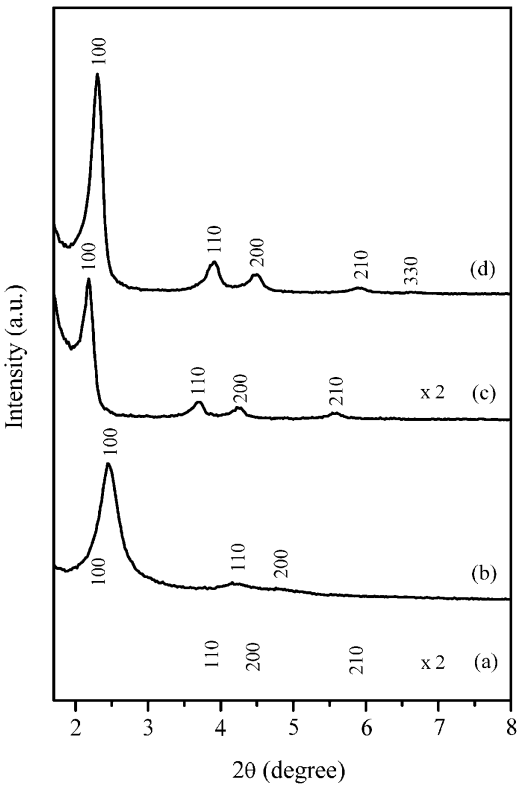

Fig. 1. Powder X-ray diffraction patterns of the prepared Si-MCM-41: (a) as-synthesized, (b) calcined and Ce-MCM-41: (c) as-synthesized, (d) calcined.

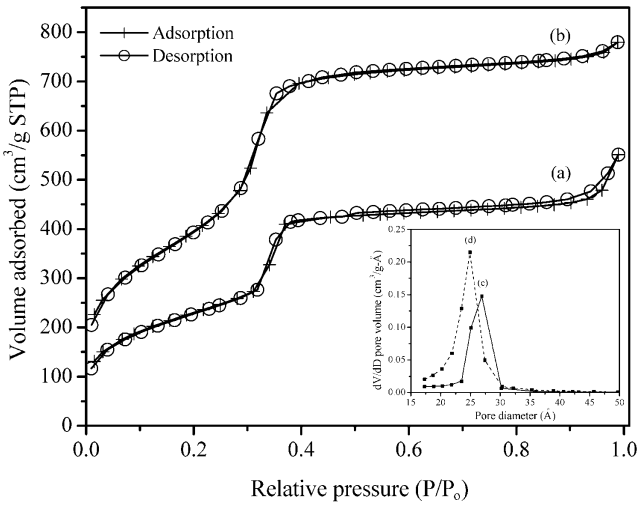

Fig. 2. N_2 adsorption-desorption isotherm at 77 K for (a) Ce-MCM-41 and (b) Si-MCM-41. The inset shows the corresponding pore size distributions for (c) Ce-MCM-41 and (d) Si-MCM-41.

the uniform tubular channels with regular hexagonal array can be seen clearly as similar to the micrograph of Si-MCM-41. The lattice cell unit, a_o, and the wall thickness measured from TEM morphology are very close to the values listed in Table 1. The tubular grain of Ce-MCM-41 with a length of about 3 μm is also observed by SEM, as can be seen in Fig. 3(b).

Fig. 4 exhibits the infrared spectra of the calcined Ce-MCM-41 and Si-MCM-41. The vibration band at 1090 cm^{-1} for Si-MCM-41 is assigned to ν_{as}(Si-O-Si) and it shifts to 1082 cm^{-1} for Ce-MCM-41. The wavenumber of this band shifting toward the lower value can be considered as an indication for the incorporation of Ce into the MCM-41 framework.[13] The IR peak appearing at about 965 cm^{-1} has been used for identifying the framework-incorporated ion.[25] Therefore, a similar shift for Si-MCM-41 at 962 cm^{-1} toward 970 cm^{-1} for Ce-MCM-41 is also observed.[13] Although the peak intensity does not show much difference, it is still evident that there is the isomorphous substitution of Si by Ce in the MCM-41 framework. In the hydroxyl region at 3000-4000

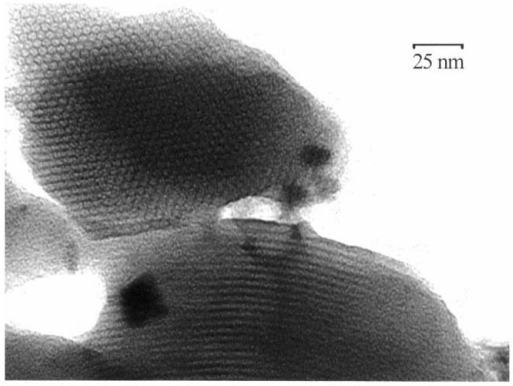

(a)

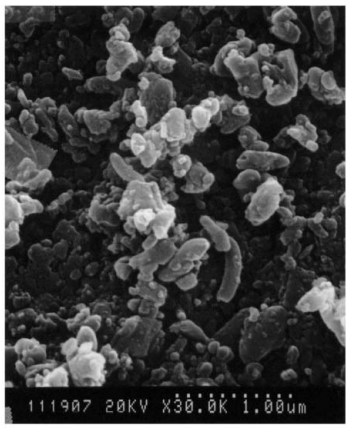

(b)

Fig. 3. Electron micrographs of the calcined Ce-MCM-41: (a) TEM and (b) SEM.

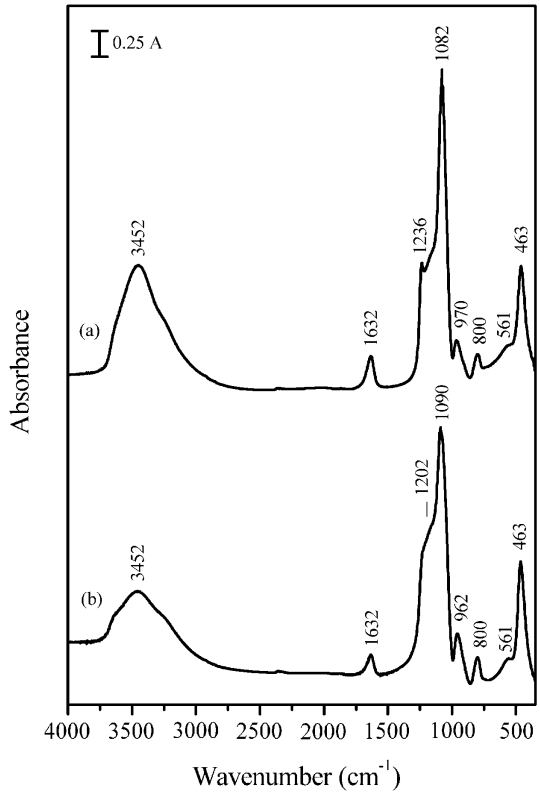

Fig. 4. Infrared spectra of the calcined (a) Ce-MCM-41 and (b) Si-MCM-41.

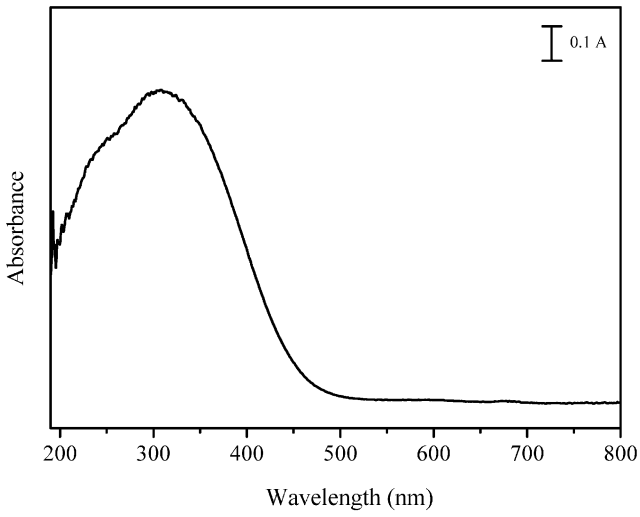

Fig. 5. The diffuse reflectance UV-visible spectra of the calcined Ce-MCM-41.

cm^{-1}, the intensity of the broad band centered at 3452 cm^{-1} for Ce-MCM-41 is apparently greater than that for Si-MCM-41. It may be because a part of the Ce incorporated on the MCM-41 surface, which led to more adsorption of hydroxyl group.

Fig. 5 shows the diffuse reflectance UV-vis spectra of the calcined Ce-MCM-41 samples. The UV-vis spectrum of Ce-MCM-41 clearly displays a high intensity band below 430 nm with a maximum around 300 nm that is due to Ce-O charge-transfer.[27] Kadgaonkar et al.[17] claimed that the absorption band centered at 300 nm is due to the presence of well-dispersed tetra-coordinated Ce^{4+} species.

Fig. 6 shows the ^{29}Si MAS-NMR spectra of the synthesized Ce-MCM-41 before and after calcination. The peaks appearing at -99.7 and -110.0 ppm shifted to -102.0 and -108.8 ppm after calcination. The NMR spectra of Ce-MCM-41 are in agreement with that of Si-MCM-41.[11] The peak at -102.0 is assigned due to Q_3 ([3 Si, 1 OH] or [3 Si, 1 Ce], and the peak at -108.0 is assigned to Q_4 due to the nonequivalent Si atoms occupying different structural sites (Si surrounded by 4 Si). Apparently, Q_4/Q_3 was increased after calcination. It is in agreement with the results of Beck[3] and Davis[28] due to the condensation of Si-OH for water formation.

The acidic properties of the synthesized MCM-41 molecular sieves were investigated by in-situ FT-IR spectroscopic studies of pyridine adsorption. The results are given as shown in Fig. 7. The pyridine adsorption was carried out under 1 torr vapor of pyridine at 150 °C for an hour, the IR spectra were taken after evacuating at room temperature for 10 minutes. Infrared spectra of pyridine adsorption show that both Ce-MCM-41 and Si-MCM-41 possess no Brönsted acidity, as no peaks appeared at 1545 cm^{-1}. Weak Lewis acidity was observed for Ce-MCM-41 with a shoulder peak of 1445 cm^{-1} and weak peaks at 1577 and 1490 cm^{-1}. There appear strong hydrogen-bonded pyridines at 1596 cm^{-1} and a shoulder peak at 1438 cm^{-1} on both Ce-MCM-41 and Si-MCM-41. The results indicated that the incorporation of Ce in MCM-41 framework resulted in a stronger Lewis acidity on the surface of the catalyst in comparison with the unmodified MCM-41.

For the catalytic activity measurements of Ce-MCM-41

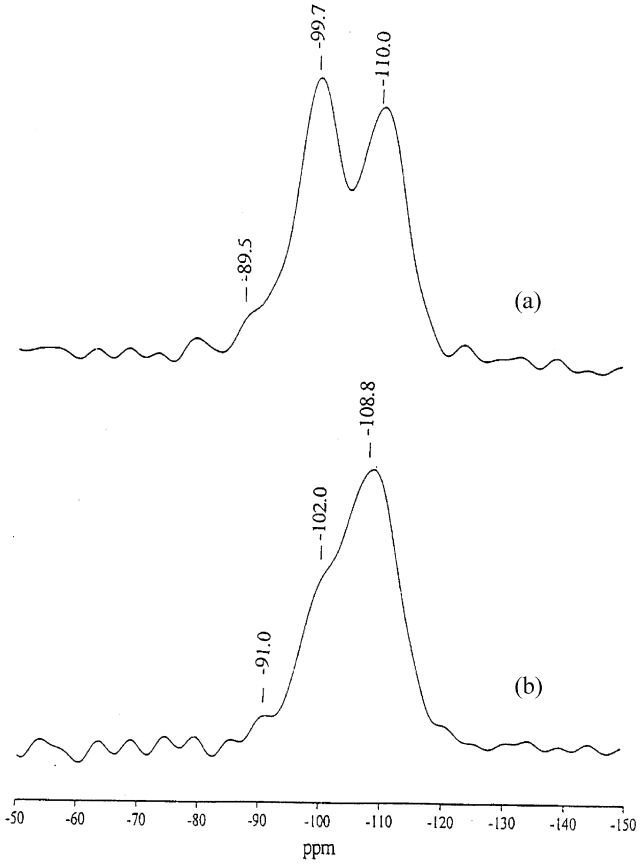

Fig. 6. ^{29}Si MAS NMR spectra of Ce-MCM-41 (a) before and (b) after calcination.

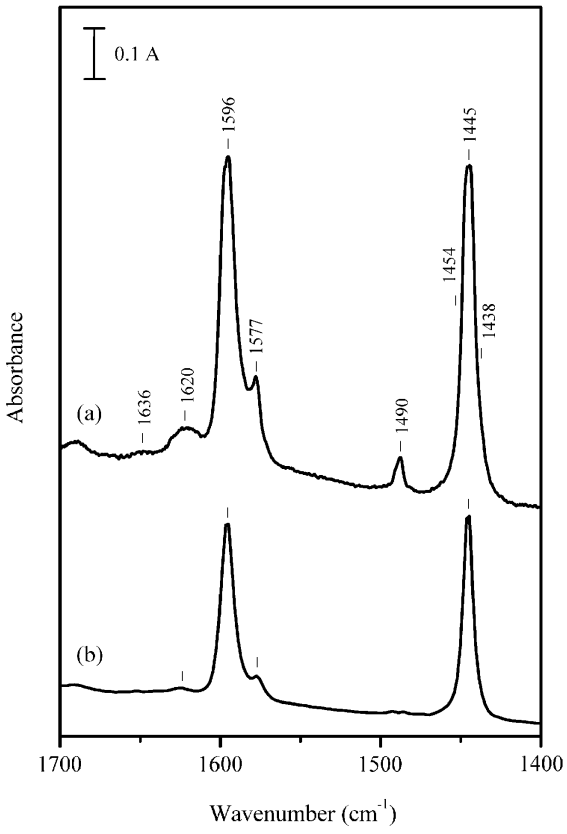

Fig. 7. In-situ FT-IR spectra of pyridine adsorption on (a) Ce-MCM-41 and (b) Si-MCM-41.

supported Rh catalyst, the NO/CO reactions were carried out in a flow-mode microreactor system with a flow-rate ratio of NO/CO = 1. A TCD detector and a quadrupole mass spectrometer were simultaneously used to detect the reaction products. Prior to NO/CO reaction, the catalyst underwent reduction in hydrogen at 500 °C for 1 hour. Fig. 8 shows the results of the NO/CO reactions over 0.5 wt% Rh/Ce-MCM-41. Nearly 100% conversion of NO was obtained at a reaction temperature of 275 °C. The conversion of CO_2 increased with temperature and achieved about 95%. As the temperature increased, the selectivity of N_2O gradually increased with a maximum at 275 °C and then decreased with temperature. The results implied that N_2O might act as the intermediate in a NO/CO reaction. It is noticeable that the catalytic activity of Rh/Ce-MCM-41 is much higher than that of the Rh/Si-MCM-41. Furthermore, the high catalytic activity of Rh/Ce-MCM-41 could be retained for several times to repeat the reactions, which indicated that cerium could facilitate the catalyst regeneration after the reactions.

The detail adsorption and reaction of NO and CO over Rh/Ce-MCM-41 catalyst was carried out by the in-situ IR spectroscopic studies. The results are shown in Fig. 9. In general, the adsorption of NO is comparatively weak. Upon the admission of 2 torr NO, there appeared very weak NO adsorption bands at 1737 and 1830 cm^{-1} due to gem-dinitrosyls, $Rh^{+}(NO)_2$.[29,30] Gaseous NO at 1876 cm^{-1} and traces of gas phase N_2O at 2224 cm^{-1} were significantly detectable. The peak at 1636 cm^{-1} was attributed to the adsorption of water on the catalyst surface. Subsequently, 2 torr of CO was admitted onto the preadsorbed NO species, resulting in IR bands at 2030 and 2117 cm^{-1} arising from gem-dicarbonyl adsorption, $Rh^{+}(CO)_2$.[29,30] As the temperature increased, the peak of adsorbed NO decreased and the peak of adsorbed CO increased simultaneously. It is evident that CO competes with the same active sites as NO. The gaseous NO and CO gradually decreased while the temperature increased. The gaseous N_2O increased with a maximum at 300 °C and then decreased with temperature. It indicates that N_2O acted as the intermediate in the NO/CO reaction, which is also evident in flow-mode reaction. The IR peak of CO_2 increased with temperature up to 500 °C. The final products of N_2 and CO_2 were analysed with

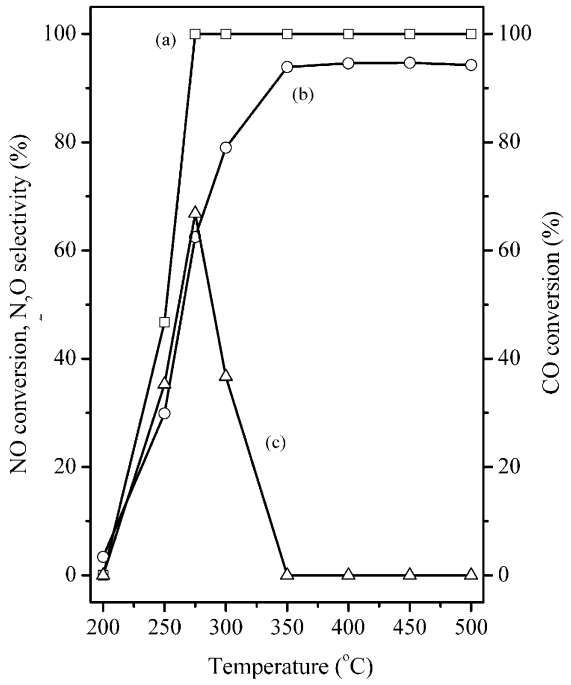

Fig. 8. The catalytic activity of NO/CO reaction over 0.5 wt% Rh/Ce-MCM-41: (a) NO conversion, (b) CO conversion and (c) N_2O selectivity.

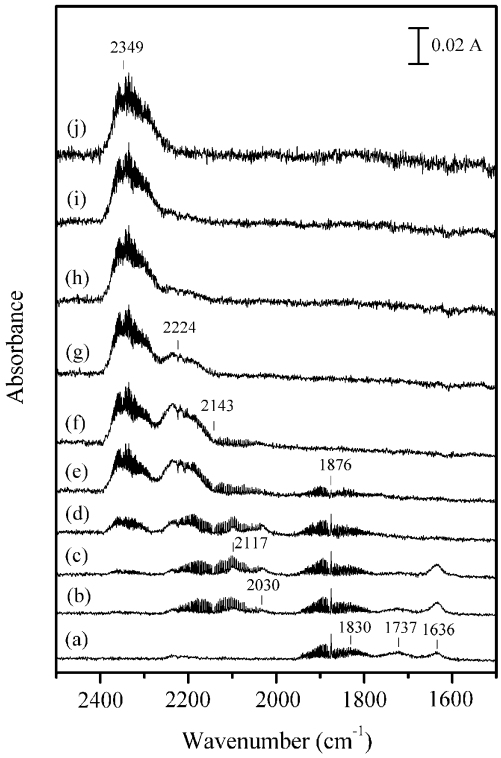

Fig. 9. IR spectra of NO/CO reactions over Rh/Ce-MCM-41: (a) after admission of 2 torr NO, (b) after admission of 2 torr CO and then the temperature was increased to (c) 100 °C, (d) 200 °C, (e) 275 °C, (f) 300 °C, (g) 350 °C, (h) 400 °C, (i) 425 °C and (j) 500 °C at a rate of 5 °C/min.

a quadrapole mass residual gas analyser. The results indicate that the adsorbed NO and CO species were catalytically reacted by Rh/Ce-MCM-41 to form N_2 and CO_2 through the intermediate N_2O.

CONCLUSIONS

We have successfully synthesized mesoporous Ce-incorporated MCM-41 by direct hydrothermal method. The low-angle XRD patterns revealed the typical five major peaks of MCM-41 type hexagonal structures. The interplanar spacing d_{100} = 38.4 Å was obtained that can be indexed on a hexagonal unit cell parameter with a_o = 44.3 Å which was larger than that of pure siliceous MCM-41 (Si-MCM-41). Transmission electron micrographs show the regular hexagonal array of uniform channel characteristics of MCM-41. The results indicated that cerium was successfully incorporated in the MCM-41 molecular sieves. Ce-MCM-41 possesses a greater unit cell parameter and pore diameter than pure siliceous MCM-41. The acidity of the MCM-41 molecular sieve is improved apparently by the presence of cerium. Rh (0.5 wt%) catalyst supported on Ce-MCM-41 exhibited very high activity for the NO/CO reactions. The Ce component acted as a promoter of the catalyst in NO/CO reactions; it enhanced the catalytic activity, prevented the catalyst from deactivation and facilitated the catalyst regeneration after the reactions.

ACKNOWLEDGEMENTS

We gratefully acknowledge the financial support from Academia Sinica, the National Science Council of the Republic of China and the Chinese Petroleum Corporation and would like to thank the technical staff in the Precision Instrument Center of the National Science Council of the Republic of China for helping in part of the experiments.

Received February 21, 2005.

REFERENCES

1. Krishna R. M.; Kevan, L. *Phys. Chem. Chem. Phys.* **2001**, *3*, 5348.
2. Shieh, D. L.; Tsai, C. C.; Chen, C. W.; Ko, A. N. *J. Chin. Chem. Soc.* **2003**, *50*, 853.
3. Corma, A. *Chem. Rev.* **1997**, *97*, 2373.
4. Beck, J. S.; Vartuli, J. C.; Roth, W. J.; Leonowicz, M. E.; Kresge, C. T.; Schmitt, K. D.; Chu, C. T.-W.; Olson, D. H.; Sheppard, E. W.; McCullen, S. B.; Higgins, J. B.; Schlenker, J. L. *J. Am. Chem. Soc.* **1992**, *114*, 10834.
5. Kresge, C. T.; Leonowicz, M. E.; Roth, W. J.; Vartuli, J. C.; Beck, J. S. *Nature* **1992**, *359*, 710.
6. Selvam, P.; Bhatia, S. K.; Sonwane, C. G. *Ind. Eng. Chem. Res.* **2001**, *40*, 3237.
7. Lin, H. P.; Mou, C. Y. *Science* **1996**, *273*, 765.
8. Lin, H. P.; Cheng, S.; Mou, C. Y. *Microporous Mater.* **1997**, *10*, 111.
9. Lin, H. P.; Kuo, C. L.; Wan, B. Z.; Mou, C. Y. *J. Chin. Chem. Soc.* **2002**, *49*, 899.
10. Lin, H. P.; Cheng, Y. R.; Lin, C. R.; Li, F. Y.; Chen, C. L.; Wong, S. T.; Cheng, S. F.; Liu, S. B.; Wan, B. Z.; Mou, C. Y.; Tang, C. Y.; Lin, C. Y. *J. Chin. Chem. Soc.* **1999**, *46*, 495.
11. Chien, S. H.; Huang, K. C.; Kuo, M. C. *Stud. Surf. Sci. Catal.* **2004**, *154*, 2786.
12. Carvalho, W. A.; Varaldo, P. B.; Wallau, M.; Schuchardt, U. *Zeolites* **1997**, *18*, 408.
13. Jeon, J. Y.; Kim, H. Y.; Woo, S. I. *Appl. Catal. B-Environ.* **2003**, *44*, 311.
14. Laha, S. C.; Mukherjee, P.; Sainkar, S. R.; Kumar, R. *J. Catal.* **2002**, *207*, 213.
15. Araujo, A. S.; Jaroniec, M. *J. Coll. Interf. Sci. Sci.* **1999**, *218*, 462.
16. Antochshuk, V.; Araujo, A. S.; Jaroniec, M. *J. Phys. Chem. B* **2000**, *104*, 9713.
17. Kadgaonkar, M. D.; Laha, S. C.; Pandey, R. K.; Kumar, P.; Mirajkar, S. P.; Kumar, R. *Catal. Today* **2004**, *97*, 225.
18. Araujo, A. S.; Aquino, J. M. F. B.; Souza, M. J. B.; Silva, A. O. S. *J. Solid State Chem.* **2003**, *171*, 371.
19. Mercuri, L. P.; Matos, J. R.; Jaroniec, M. *J. Alloy. Compd.* **2002**, *344*, 190.
20. Gandhi, H. S.; Graham, G. W.; McCabe, R. W. *J. Catal.* **2003**, *216*, 433.
21. Belzunegui, J. P.; Sanz, J. *J. Phys. Chem. B* **2003**, *107*, 11705.
22. Su, E. C.; Montreuil, C. N.; Rothchild, W. G. *Appl. Catal.* **1985**, *17*, 75.
23. Harrison, B.; Diwell, A. F.; Hallett, C. *Platinum Met. Rev.* **1988**, 32.
24. Kim, G. *Ind. Eng Chem. Prod. Res. Dev.* **1982**, *21*, 267.
25. Chien, S. H.; Chang, Y. C. *Bull. Inst. Chem. Academia Sinica* **1989**, *36*, 81.

26. Koh, C. A.; Noony, R.; Tahir, S. *Catal. Lett.* **1997**, *47*, 199.
27. Hari Prasad Rao, P. R.; Ramaswamy, A. V.; Ratnasamy, P. *J. Catal.* **1992**, *137*, 225.
28. Chen, C. Y.; Li, H. X.; Davis, M. E. *Microporous Mater.* **1993**, *2*, 17.
29. Iizuka, T.; Lunsford, J. H. *J. Mol. Catal.* **1980**, *8*, 391.
30. Arai, H. *Ind. Eng. Chem. Prod. Res. Dev.* **1980**, *19*, 507.